JOURNAL OF MATERIALS SCIENCE **39** (2004) 6473–6482

Structure-fracture measurements of particulate gels

C. ÖHGREN, M. LANGTON, A.-M. HERMANSSON*
SIK-The Swedish Institute for Food and Biotechnology, P.O. Box 5401, SE-402 29 Göteborg, Sweden
E-mail: amh@sik.se

Images on a micron scale and the stress-strain behaviour of gel structures during tension were simultaneously recorded in real time using a mini fracture cell under the confocal laser scanning microscope (CLSM). β-lactoglobulin gels tailor-made to vary in density, connectivity, thickness of strands and size of aggregates and clusters were used as a food model system. Amylopectin and gelatin were used to generate different types of β-lactoglobulin network microstructures and also as a second continuous phase.

Both rheological and structural differences in fragility between β-lactoglobulin gels were verified according to the density of their aggregated network structure. A dense gel has a more brittle behaviour where the clusters are rigid and the crack propagates smoothly compared to a gel with an open network structure, which has a discontinuous crack growth, via a winding pathway around clusters, and also break-up of the pores far from the crack tip. Differences in the stretchability of the aggregated β-lactoglobulin structure, induced by addition of amylopectin solution, were proved and related to differences in stress-strain behaviour and crack propagation.

Gelatin gels in the pores between the β-lactoglobulin clusters do not affect the structure of the β-lactoglobulin network but make the fracture fragile giving a smooth fracture surface, cause continuous crack growth and fracture propagation through β-lactoglobulin clusters. This is a consequence of that the mixed gel follows the behaviour of the gelatin gel when the gelatin phase is stronger than the β-lactoglobulin network.

1. Introduction

The perceived texture of food depends to a large extent on the initial stages of fracture in the microstructure. Studies of the fracture behaviour of microstructures provide valuable information on the forces keeping the structures together, required when attempting to design appropriate structures. A challenging problem is to control the texture, as this is largely determined by structural rearrangements during deformation and fracture. The correlation between the results of rheological measurements and conventional microstructural data is not always unambiguous. This has led to a demand for new types of rheological measurements as well as microstructural measurements. Research tools have gradually become available that enable us to deal with the complexity of food systems. Measuring cells can be adapted to the confocal laser scanning microscope, allowing us to directly follow structural changes during application of stress.

Real-time measurements of structure and consistency provide a unique opportunity to explore food characteristics. A few articles have been published describing mechanical measurements obtained during simultaneous imaging of food systems [1–3]. Thiel *et al.* [3] demonstrated the use of enviromental scanning electron microscopy (ESEM) for *in situ* observations during mechanical testing of carrots. Structural rearrangements observed were crack propagation and cell wall distortion in real time related to stress-strain characteristics. Stokes *et al*. [2] used *in situ* tests in ESEM to study breadcrumbs. Results showed that the struts and strings of matrix material, bridging the voids, were influenced by the moisture content, and that this is a determining factor in fracture propagation. Dynamic structural studies using the confocal laser scanning microscope (CLSM) were made of gelatin-maltodextrin gels by Plucknett *et al*. [1]. They observed that the interfacial fracture energy controls the fracture properties, i.e., a weak interfacial energy resulted in debonding at low strain. Stepped displacements were applied, with an image acquired after each step, to avoid stage vibrations.

By performing real-time measurements, we can measure stress-strain behaviour and microstructural changes at the same time. Accordingly, it is feasible to follow crack propagation and measure at what stress it starts and how fast the crack ruptures. No crack length

*Author to whom all correspondence should be addressed.

analyses of food material have been made previously to our knowledge, but they are frequently used with other types of materials. In most cases the crack growth rate is analysed when fatigue tests of polymers, metals, glass or other composite materials are carried out e.g., [4–6]. A structure-related cause of variations in crack rate may, for example, be seen in sintered steel, which has an inhomogeneous microstructure, consisting of a mixture of soft and hard phases, resulting in a decreased fatigue crack growth rate compared to homogeneous steel [6]. Both jagged discontinuous and continuous crack growth has been shown in fatigue tests of polyethylene in which the stress intensity was varied [4]. Microscopy observations showed that cavitations, voiding and rupture took place within an extended damage zone ahead of the crack tip when the crack growth was discontinuous under high stress intensity. Under low stress intensity, when the crack grew continuously, the influenced zone was limited to the crack tip.

Different materials fracture in different ways. For example, a potato crisp will snap immediately while soft toffee will slowly tear apart. In fracture mechanics different kinds of fractures are classified according to how brittle or ductile they are. Examples are cleavage, intergranular brittle or creep fracture, plastic growth of voids into fracture, and rupture by necking or shearing-off. Between these extremes a whole range of possibilities exists [7].

We have previously performed dynamic experiments using CLSM of mixed particulate β-lactoglobulin-amylopectin gels, using the same approach as Plucknett *et al.* [1] by stopping the extension and recording an image. The experiments showed that fracture occurred deeper inside the structure, in relation to the crack tip, for gel compositions containing pure 6% β-lactoglobulin and 6% β-lactoglobulin/0.75% high molecular weight (H_{mw}) amylopectin. These gels are weak and fall easily apart. In another composition of 6% β-lactoglobulin/2% low molecular weight (L_{mw}) amylopectin, which had a higher G′ and more sponge-like behaviour, the fracture occurred only at the crack tip. This may indicate differences in connectivity and flexibility between the clusters among the gel types [8, 9]. The result was also concordant with earlier studies with the same gel compositions, involving rheological measurements and evaluation of the microstructure of set gels [10, 11].

Many real food products exhibit aggregated phase-separated microstructures where the aggregates form a particulate network. For example, the microstructure of β-lactoglobulin or whey can be compared with that of yoghurt [12, 13]. In the present work we have used particulate β-lactoglobulin gels as the model system. Different types of aggregated phase-separated network structures were prepared, varying in density, size of pores and clusters, thickness of strands and connectivity of strands, obtained by varying the medium in which the β-lactoglobulin gel was formed: water, amylopectin solution or gelatin. (The gelatin gelled after the β-lactoglobulin network was formed.)

The present report concerns a study of simultaneous microstructural and rheological measuring methods describing the initial stage of fracture of particulate protein gels. Rheological measurements are always performed under dynamic conditions. To obtain equivalent information from microstructural data in this study, we have monitored the microstructure of gels during successive deformation under a confocal laser scanning microscope. The purpose of the study was to find out what structural rearrangements occur during the deformation of particulate β-lactoglobulin microstructures and, at the same time, to characterise the initial stage of fracture rheologically in order to establish structure-rheology relationships.

2. Experimental procedures

2.1. Materials

The materials used were natural amylose-free amylopectin starch from potato (pap) developed by Lyckeby Stärkelsen and Svalöf Weibull using genetic engineering. β-lactoglobulin (β-lg), WPI PSDI-2400, was obtained from MD Food Ingredients, Denmark. A detailed description of the materials is given elsewhere [10]. The acid-processed, granular-formed gelatin used was obtained from Extraco, Klippan, Sweden and had a nominal strength of 250 Bloom. All calculations in this study were done on a dry matter basis, and all concentration values stated in % refer to wt%.

2.2. Sample preparation

The β-lg was dissolved in distilled water, pH adjusted to 5.4, degassed and poured into moulds of aluminium with squared cross-sections of 13 × 13 mm. The ends were closed with heat-proof tape (scotch 425). The moulds were greased to prevent the samples from sticking to the walls. The samples were then placed in a FP40-MS Julabo programmable silicon oil bath (Julabo Labortechnik GmbH, Seelbach, Germany). The temperature was increased to 90°C at a heating rate of 2.5°C/min and held at 90°C for 1 h. Thereafter the temperature was decreased to 20°C at a cooling rate of 2.5°C/min. The samples were stored overnight, 15–18 h, at a temperature of 20°C.

In the mixed gel case, the biopolymers were dissolved separately at double concentrations and then mixed. Pap was mixed with distilled water and the dispersion was heated to 120°C, to fully dissolve the granule remnants, and then cooled at room temperature (20°C). The molecular weight of this solution was 5×10^7 Da (H_{mw}) [14]. The molecular weight of the pap solution was reduced to approximately half the value of the H_{mw} pap by shearing it in a homogenizer, Ultra Turrax, T25, (IKA®-labortechnik, JANKE & KUNKEL, Staufen, Germany), at a rate of 20500 min^{-1} for 1 min, denoted L_{mw}. The gelatin was dissolved in distilled water at 50°C before mixing it with the β-lg solution.

2.3. Structure-fracture measurements

The samples were cut into 10 mm-long test pieces, and a notch was cut perpendicular to the applied force direction along one side of the test pieces at a depth of

1 mm. Pure β-lg and mixed β-lg/pap gels were stained with a droplet of 0.01% Texas Red solution, which has a fluorescence maximum at ~620 nm. The gelatin-containing samples were added 0.025% Rhodamin solution (1:25) (fluorescence maximum at ~602 nm) during the mixing step, because these gels were so tight that the colouring matter could not push through. The test pieces were glued to sandpaper-covered clamps in a Microtest miniature material tester (Deben, Suffolk, UK). The Microtest was then placed under a confocal laser scanning microscopy (CLSM) Leica TCS SP2 (Leica Ltd., Heidelberg, Germany). The light source was HeNe lasers using $\lambda_{ex} = 594$ nm (Texas Red) and 543 nm (Rhodamin). The microscope objectives used were air-objectives having a magnification of 5 × (a 2 × zoom was used) when following the fracture path and 10 × (8× zoom) when recording ahead of the notch tip, and a numeric aperture of 0.12 and 0.30, respectively. Images were taken each 1.629 s, and the section 20 μm down in the sample was monitored. A constant tensile speed of 0.66 mm/min was applied, while force and extension were measured. It was important to make a notch to control the fracture. Without a notch most of the samples fractured in one of the glued sides.

The crack propagation was determined by measuring the prolongation of the notch in the images. The crack length was used to calculate the prevailing area, which was necessary for determining the true stress.

The experiments are highly reproducible when everything in the preparation works satisfactory. In many of the tests, especially for gels containing low concentrations of protein, the gel pieces fractured in the glued sides instead of in the notch because the gels are very weak and sensitive for pushes under the attach-stage. At least three entirely succeeded experiments were made on each sample.

3. Results and discussion

Real-time dynamic video recording of gels under simultaneous stress-strain exposure has been shown to work satisfactorily. The mini fracture cell moves very smoothly and few vibration disorders have been observed. However, because we observed structural changes during deformation at a high magnification up to ~80×, a great deal of concentration was needed during the performance since the gel microstructure was moving in both an x-y direction and in a z direction while the sample was being deformed. The same piece of microstructure, which only has a size of 190 μm × 190 μm for the highest magnification, has to be studied during the whole measurement, and therefore it is necessary to adjust the stage in these directions in small steps during the performance.

In this investigation we have chosen to study how a crack propagates from a notch as a starting point. We have used a low magnification and a large pinhole, so a large segment of the gel piece can be monitored in both an x-y and a z direction. In addition, we have followed the alterations of small structure components ahead of the notch tip by using a high magnification and a small pinhole. The stress-strain behaviour was measured continuously while the microstructural changes were photographed.

The studied β-lg microstructures have been designed and chosen according to criteria such as density, homogeneity and connectivity. Furthermore, the ambient medium has been varied between water, amylopectin solution and gelatin gel. The ambient medium was varied both in order to generate the desired network structures and to investigate the influence of different media in the pores created by the β-lg networks.

3.1. β-lactoglobulin gel-structures varying in density

Pure β-lg gels of varying concentrations were investigated in order to generate gels that differed in the density of the β-lg aggregated networks. Fig. 1a and c show CLSM images of unaffected microstructures of 6 and 12% β-lg gels. The gel with the higher concentration has a denser β-lg gel network (white in the image) with small pores (black in the image) compared to the gel containing 6% β-lg. Fig. 1b and d show how the same microstructures are altered when they are exposed to maximum deformation after tension at a rate of 0.66 mm/min. The images are taken when the stress is at its maximum and the crack has almost reached the photographed section. The size of the images is adjusted so that exactly the same structure components are shown both before and after the deformation. Clear changes are shown for the gel with a lower concentration, see Fig. 1a and b. Most of the pores have grown in the deformation direction. For example, the pore in the marked area has grown considerably. It is also possible to see how whole clusters have turned in the deformation direction, see the cluster in the marked region in Fig. 1a and b. A comparison of Fig. 1c and d shows few changes. However, the size of the images indicates that the total structure has been longer in the x direction and shorter in the y direction. Nevertheless, if the two marked regions are compared, it is evident that more small pores have been formed and that the larger pores have been somewhat extended in the x direction and compressed in the y direction.

These two different types of behaviour depending on the density of the aggregated microstructure probably reflect the brittleness of the gels. This can be confirmed since stress and strain were measured during the same experiment. The fracture parameters are shown in Fig. 2, where the dense and firm gel containing 12% β-lg has a ~6 times higher σ_b, stress at break than the more open and soft gel containing 6% β-lg, which, on the other hand, can be stretched longer. Furthermore, the start of lengthening of the notch and crack propagation is shown for both gel types. Before the start of crack propagation no new local fractures are observed in the microstructure at the magnifications studied apart from widening of the existing ones. The crack propagation behaves similarly in relation to the stress maximum for both gel types. However, crack growth differs in appearance; it is represented by a smooth curve in the stronger gel, while in the weaker gel crack propagation is more step-wise, probably as a result of the more

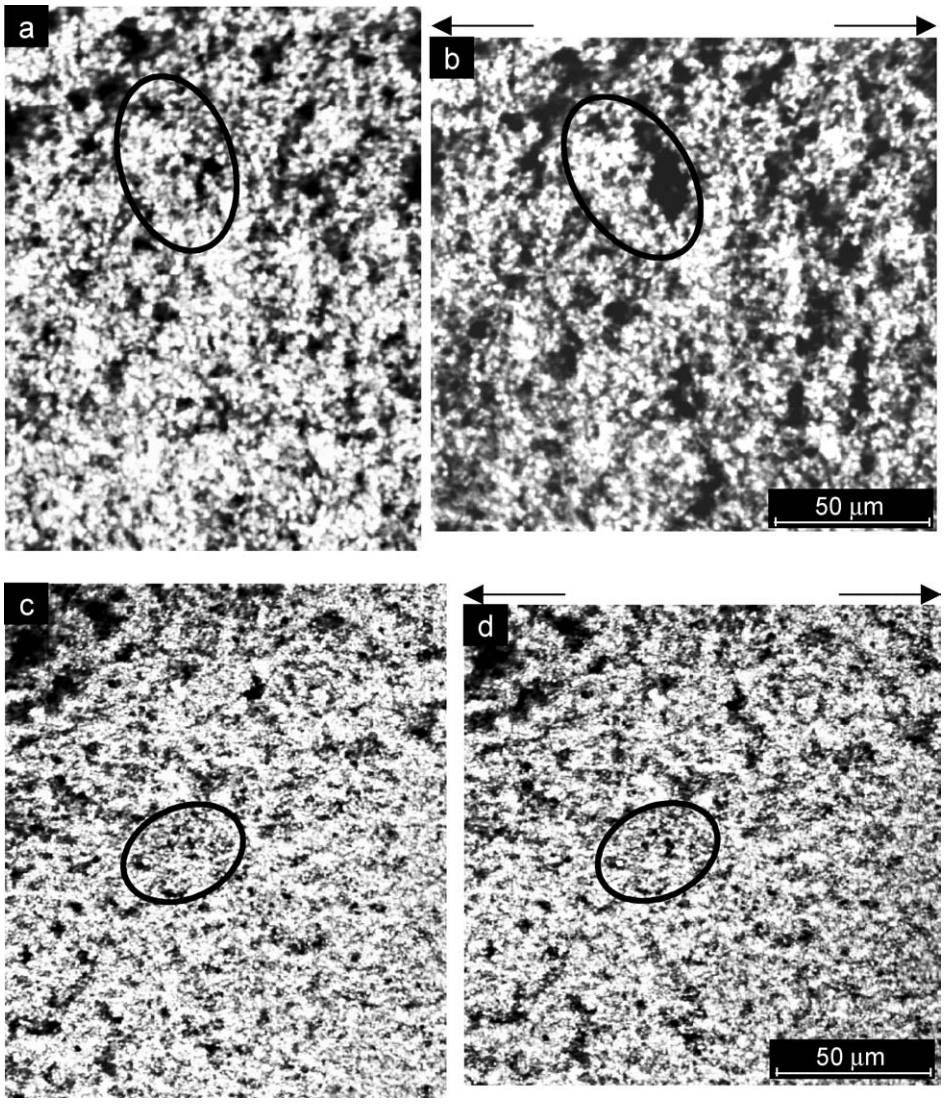

Figure 1 A 6% and a 12% β-lg gel before (a, c) and at maximum deformation (b, d). Examples of the changes in pore size and alteration in the direction of clusters are marked in the images.

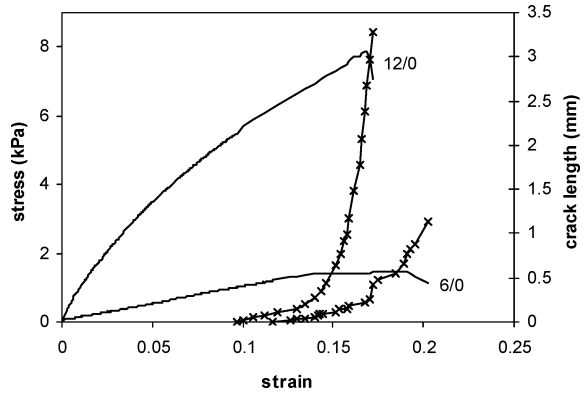

Figure 2 Stress and crack length versus strain for gels containing 6 and 12% β-lg.

open, or less dense, microstructure of the 6% β-lg gel. The step-wise crack growth is a consequence of fewer connections between clusters, explaining why steps became larger between locations that can resist stress.

Tensile deformation of particle gels resembling food systems such as yoghurt and cheese has recently been studied by Rzepiela [15] using Brownian Dynamics simulations. The gels were found to exhibit ductile fracture rather than yielding and maintaining the structure. Simulated structural images showed that the whole gel piece was extended in one direction and shrunk in the perpendicular direction during deformation. An inherent notch in the structure grew in the early stages of deformation in the extension direction and changed shape. Later, both the thickness and length of the notch increased due to joining of smaller voids. These findings seem to fit what really happens when comparing them with our results with β-lg gels. However, the model also shows that the resulting fracture was due to global material fracture rather than crack propagation from a notch, which is not in agreement with our results. Nor did the stress-strain response correspond to our findings: after the stress maximum a period was reached when the stress decreased slowly (more slowly than it increased from the beginning), unlike our measurements where the stress decreased rapidly after the stress maximum. The model incorporated soft spherical particles and reversible flexible bond formation.

3.2. Pap-containing β-lactoglobulin gel-structures varying in connectivity

The appearance of the β-lg particulate network in the presence of pap solution with varying molecular weight

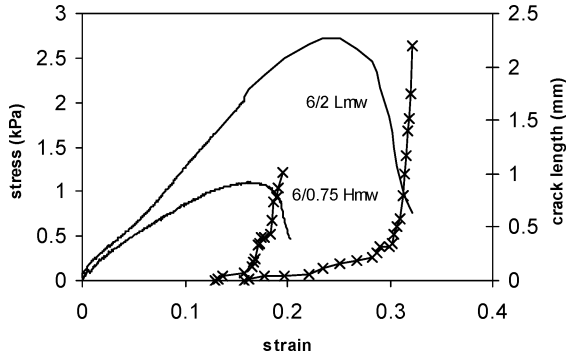

Figure 3 Stress and crack length versus strain for mixed gels containing 6% β-lg/ 0.75% H_{mw} pap and 6% β-lg/ 2% L_{mw} pap.

has been thoroughly investigated previously [8–11, 14]. Fig. 3 shows stress and crack length versus strain for mixed gels containing 6% β-lg/0.75% H_{mw} pap and 6% β-lg/2% L_{mw} pap, respectively. The stress-strain behaviour of the weaker gel containing 6% β-lg/0.75% H_{mw} pap is similar to that of a pure 6% β-lg gel, see Fig. 2. The crack growth starts around the same strain and accelerates in a similar pattern to the pure 6% β-lg gel when the stress has reached maximum. Since the gel containing 6% β-lg/0.75% H_{mw} pap has a low strain at break, it results in a short period of slow crack growth. Soon after the notch has started to crack at the tip, the whole structure behind the notch-tip splits. The simultaneously photographed microscopy images show this rigid and "falling apart" behaviour in Fig. 4. Fig. 4a shows the structure of the gel containing 6% β-lg/75% H_{mw} pap at the start of deformation and Fig. 4b the structure just before it falls apart. The clusters behave inflexibly and do not change much during the pulling. The pattern in the marked region shows that the connections between loosely connected small aggregates inside larger clusters burst and small pores become larger.

The behaviour of the stronger gel containing 6% β-lg/2% L_{mw} pap is different. The stress-strain curve has a tendency to show more s-shaped behaviour compared to the more r-shaped stress-strain behaviour of the other gel type, which is shaped like the letter r with a decreasing slope. An s-shaped curve indicates yielding of the material when the slope decreases and the curve has a sigmoidal behaviour [16]. This somewhat rubber-like behaviour is common for certain types of foods with high moisture content. For example, a similar stress-strain curve has been shown for sponge cake and young Gouda cheese exposed to compression [17, 18]. The curve form may also be influenced by the strain rate [17]. The behaviour is in concordance with the corresponding micrographs; see Fig. 5a and b where Fig. 5a shows the unaffected microstructure and Fig. 5b the extended microstructure at maximum stress. The gel containing 6% β-lg/2% L_{mw} pap is composed of flexible strands and clusters, i.e., the network components have the ability to deform and stretch out in the deformation direction without rupturing. Notice also that the structure has not cracked at any position but has merely been stretched out. The crack starts earlier, in relation to the stress maximum, for the gel containing 6% β-lg/2% L_{mw} pap but has a long period where it develops slowly and does not accelerate in length before the maximum in stress has passed.

Both gel types exhibit a somewhat discontinuous, step-wise, crack growth probably as a consequence of asymmetric stress-holding connections, since the microstructure is rather inhomogeneous. The difference in crack propagation is more clearly presented in Fig. 6, where the stress is plotted versus the crack length. The graph shows the stress at which the crack growth accelerates and the sample starts to split. The start of sample split acceleration occurs where the curve becomes horizontal, i.e., when the crack propagates a long distance at constant stress. It is shown that the gel containing 6% β-lg/0.75% H_{mw} pap starts to accelerate in sample split at the stress maximum while the gel containing 6% β-lg/2% L_{mw} pap does not start until after the maximium in stress because the 6% β-lg/2% L_{mw} pap-containing gel is formed of more flexible strands, which can be deformed considerably without rupturing. This means that this structure has a rubbery behaviour, since it does not fall apart when the stress is at a maximum but

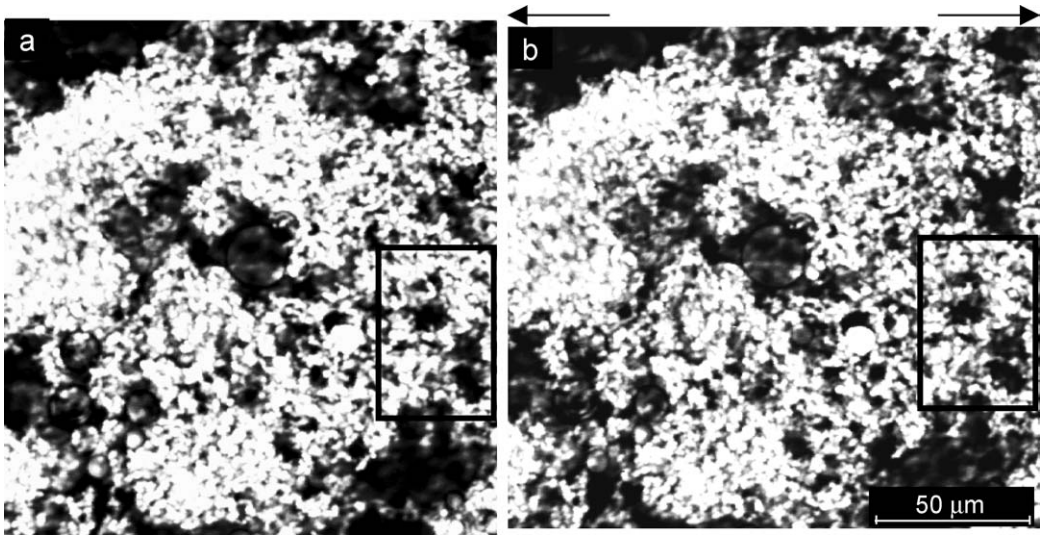

Figure 4 A mixed 6% β-lg/0.75% H_{mw} pap gel before (a) and at maximum deformation (b). An example of changes in pore size is marked in the images.

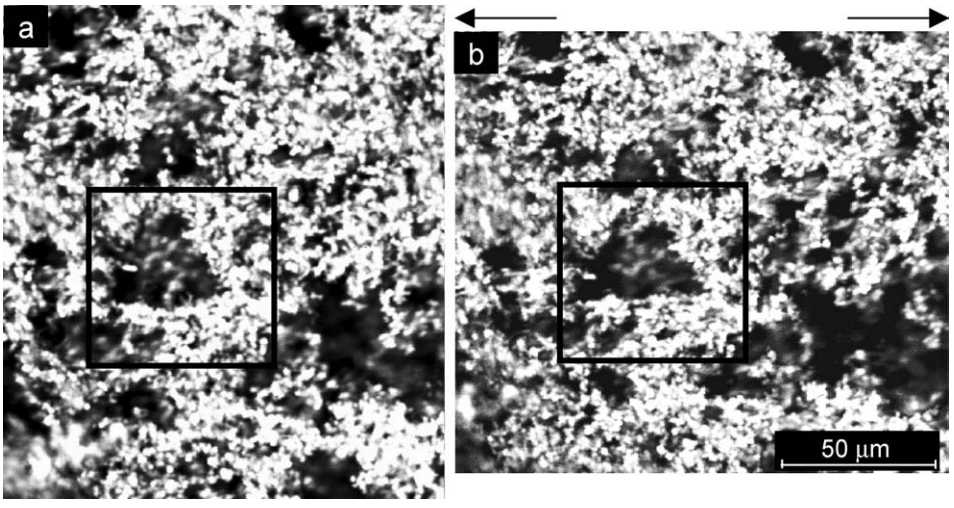

Figure 5 A mixed 6% β-lg/2% L_{mw} pap gel before (a) and at maximum deformation (b). Examples of the changes in pore size and the extension of the clusters are marked in the images.

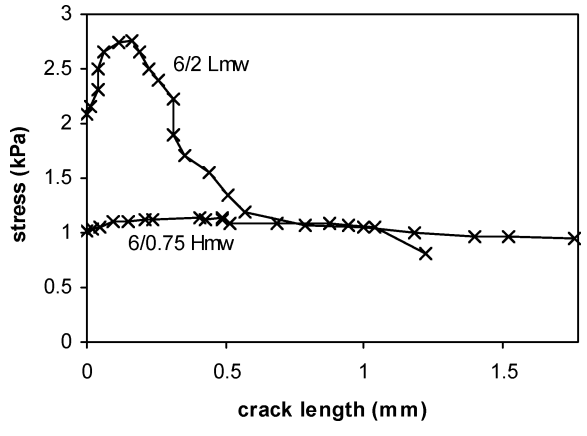

Figure 6 Stress versus crack length for mixed gels containing 6% β-lg/ 0.75% H_{mw} pap and 6% β-lg/ 2% L_{mw} pap.

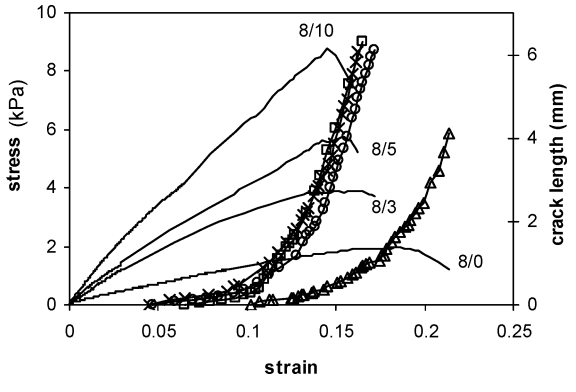

Figure 7 Stress and crack length versus strain for pure and mixed gels containing 8% β-lg, (—Δ—), 8% β-lg/3% gelatin, (—○—), 8% β-lg/5% gelatin (—×—) and 8% β-lg/10% gelatin (—□—).

will keep together and not fracture before it has been deformed considerably.

When comparing the results of the gels containing amylopectin with earlier studies on these gels [10], it is shown that the stress at break is in agreement but not always the strain at break. This is a consequence of the different beahviours of the structures of the gel types depending on variation in strain rate.

3.3. β-lactoglobulin gel-structures incorporated in gelatin gels

Gelatin was the third medium in which particulate β-lg was allowed to form a gel. The gelatin forms a fine-threaded gel on cooling between the heat-induced particulate β-lg strands without changing the particulate structure. The microstructure and the rheological behaviour of mixed β-lg gelatin gels have previously been studied thoroughly by Walkenström *et al*. [19], but not at the initial stage of fracture. It appeared that the extension at fracture of a 8% β-lg gel with a 1% gelatin addition (not shown) followed the behaviour of the pure 8% β-lg gel, but addition of 3, 5 and 10% of gelatin resulted in shorter strain at fracture, see Fig. 7. The mutual relations between the samples were similar for the stress at break; the pure 8% β-lg gel and the gel containing 1% gelatin had the same behaviour, while gels containing 10% gelatin were stronger than the gels containing 5% gelatin, which were stronger than the ones containing 3%. The studies by Walkenström *et al*. [19] showed that a transition occurred in rheological properties around the addition of 3% gelatin but that the particulate network structure was unaffected. Slow crack propagation starts earlier for gels containing 3% gelatin or more compared to pure β-lg gels, which is shown in Fig. 7. When the stress is plotted versus the crack length as in Fig. 8, it is clearly shown that gels containing 3% gelatin or more have a region where the curve levels out earlier in relation to the stress maximum, i.e., the stress continue to increase although the crack has fractured more than 2 millimetres. We can observe that the higher the gelatin concentration in the gels, during the longer crack length the stress continues to rise. For the samples containing 5 and 10% gelatin, the stress continues to rise even after crack propagation has started to accelerate.

As a comparison, mixed particulate β-lg/gelatin gels can resist fracture to a high extent but are not as flexible as a mixed particulate 6% β-lg/2% L_{mw} pap gel, in which acceleration of crack growth does not start until after the stress maximum, compare Figs 6 and 8. In the

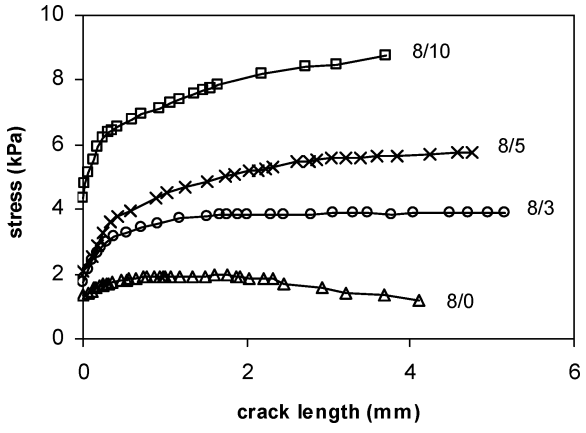

Figure 8 Stress versus crack length for pure and mixed gels containing 8% β-lg (—Δ—), 8% β-lg/3% gelatin (—◯—), 8% β-lg/5% gelatine (—×—) and 8% β-lg/10% gelatine (—□—).

CLSM images, Fig. 9, the behaviour of gels containing 8% β-lg/1% gelatin and 8% β-lg/5% gelatin can be compared in the undeformed and deformed state. Addition of 1% gelatin to 8% β-lg gel has no influence on rheological or microstructural properties. The β-lg network is still stronger than the gelatin network and the behaviour follows that of a pure 8% β-lg gel, i.e., the pores become larger and whole clusters can be displaced and split up during deformation, see Fig. 9a and b. The behaviour is alike that of the pure 6% β-lg gel, see Fig. 1a and b. In the gel containing 5% gelatin, on the other hand, no clusters have split up. Pores and clusters have only stretched out and follow the movement of the gelatin gel, see Fig. 9c and d. The marked areas in Fig. 9 are regions where the rearrangements described above are clearly shown.

3.3.1. Initial stage of crack propagation

Fig. 10 shows the initial crack propagation in CLSM micrographs for a pure 8% β-lg gel (left column) and for a mixed 8% β-lg/10% gelatin gel (right column), at a lower magnification than presented in earlier micrographs. The images at the top show the hand-made notch before the crack has started to propagate. The other images show how the structures near the notch are altered when the crack has just started to propagate from the notch. A pure 8% β-lg gel is fractured via a winding pathway. The fracture path moves between clusters and chooses the easiest passage. Fracture in the microstructure has also occurred deeper inside the structure ahead of the crack, not only at the tip of the crack. The mixed gel containing gelatin has a similar β-lg network structure to the pure β-lg gel in the undeformed state. However, during fracture, crack propagation through the β-lg clusters occurs. A more

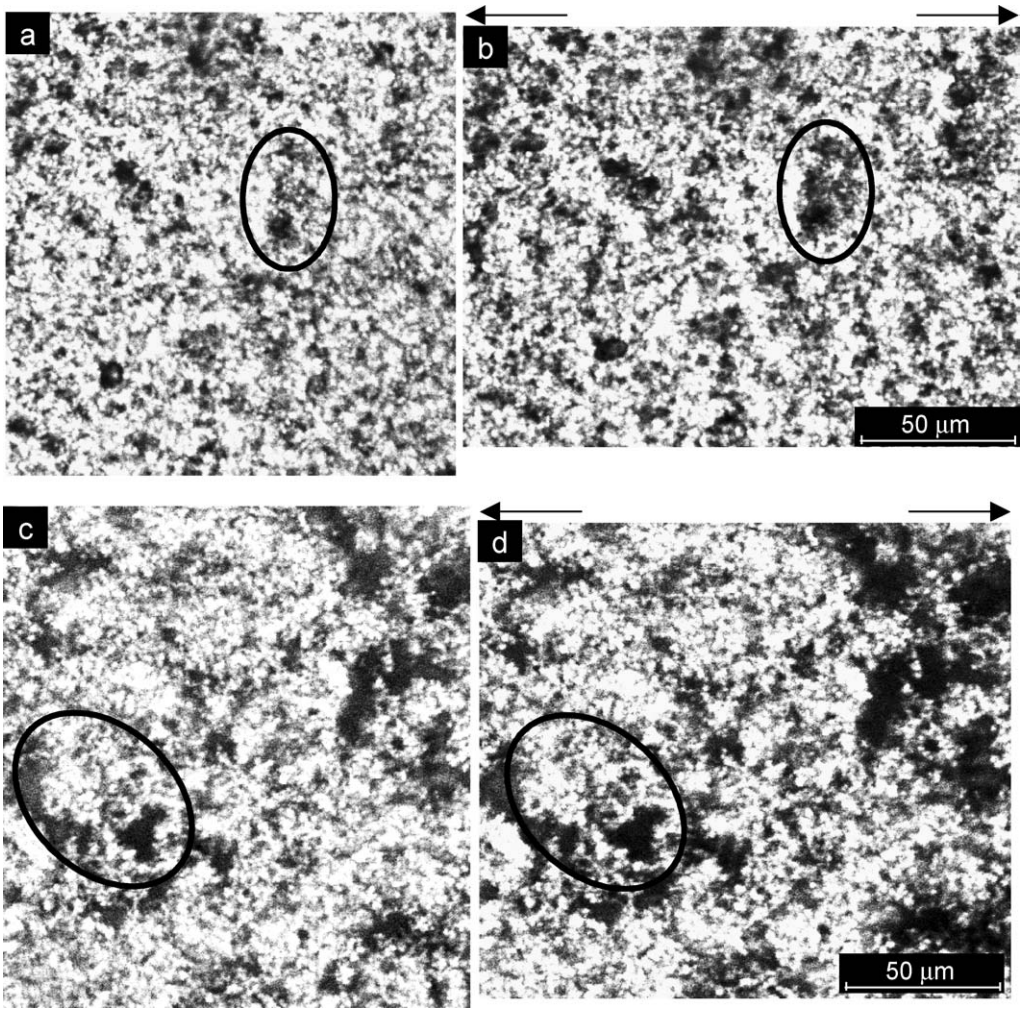

Figure 9 Mixed gels of 8% β-lg/1% gelatin and 8% β-lg/5% gelatin before (a, c) and at maximum deformation (b, d). An example of changes in pore size is marked in the images.

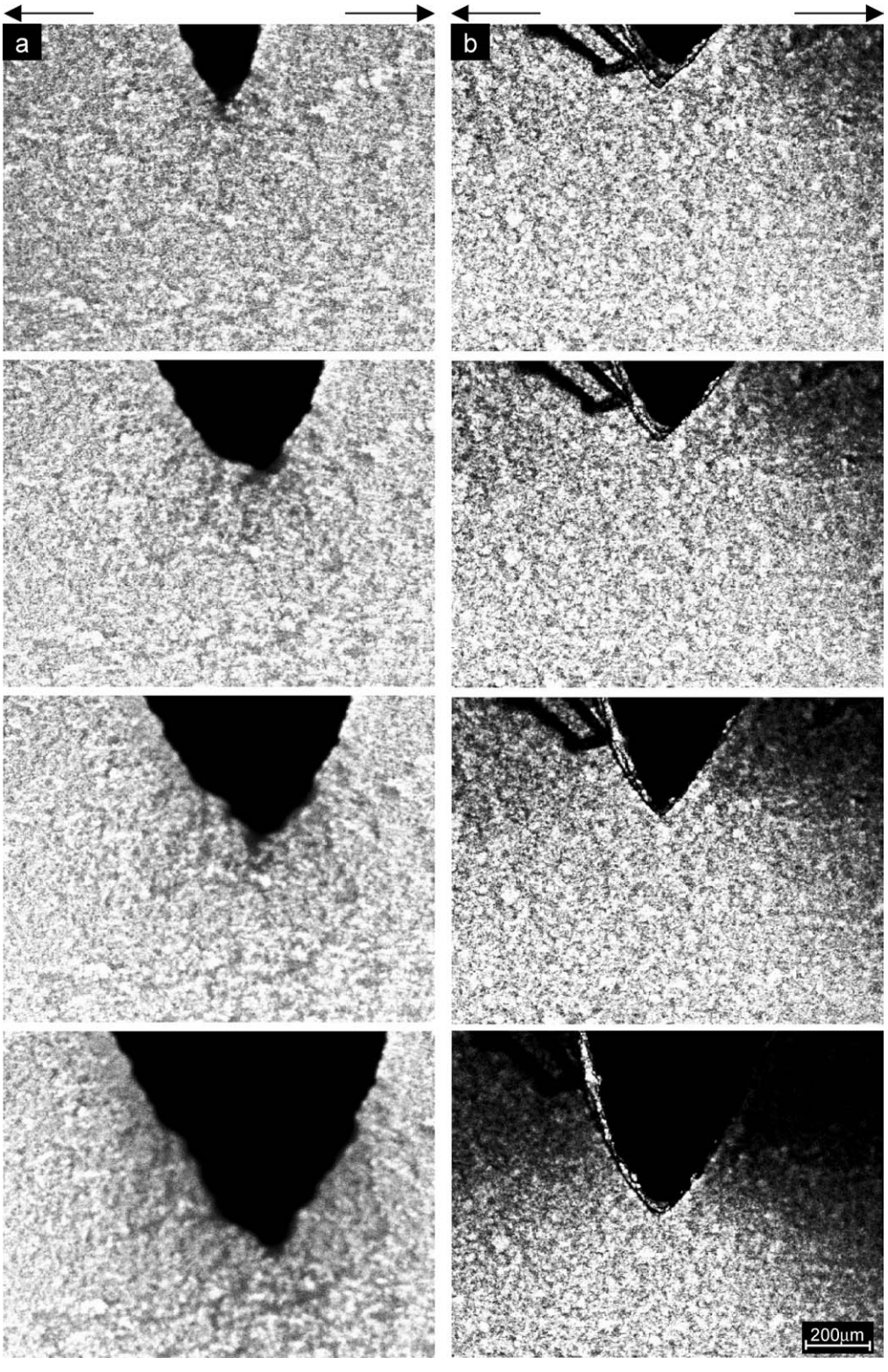

Figure 10 Pure 8% β-lg (a) and mixed 8% β-lg/10% gelatine (b) gels at the initial stage of crack propagation increase.

brittle fracture is verified compared to the pure β-lg gel. The structure deeper inside the structure is uninfluenced with respect to fracture, only the structure at the tip of the notch is fractured. Hence, the mixed gel follows the behaviour of the gelatin gel after a certain amount of added gelatin, about 3%, i.e., when the gelatin phase is stronger than the β-lg network. The fracture path of the gel containing 6% β-lg/2% L_{mw} is winding and moves between clusters similarly to the pure β-lg gel. The difference compared to the pure β-lg gels is that the structure ahead of the crack tip has not brooked-up, but like the gelatin-containing gels, just the structure at the tip of the crack is fractured.

Notice also the differences in the curvature of the notch between the two gel types when the cracks have propagated the same distance (the images at the bottom in Fig. 10). The radius of curvature of the notch in the gelatin-containing gel was less than that of the pure β-lg gel, because the pure β-lg gel was longer extended than the gelatin-containing gel.

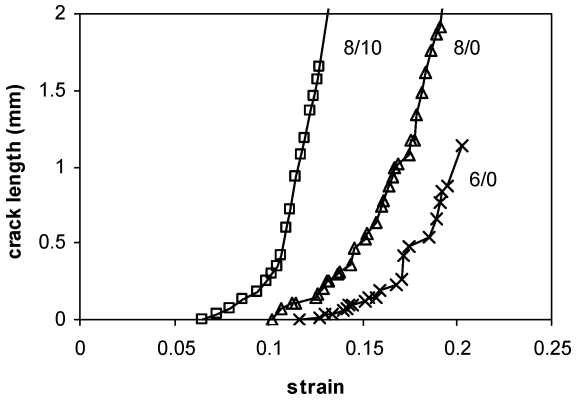

Figure 11 Crack length versus strain for pure and mixed gels containing 6% β-lg (—×—), 8% β-lg (—Δ—) and 8% β-lg/10% gelatin (—□—).

The β-lg gel which cracks via a winding pathway shows discontinous crack propagation while the gelatin-containing gel shows continuous crack propagation. Fig. 11 shows crack growth during the initial stage for the mixed 8% β-lg/10% gelatin-containing gel type and for pure 6 and 8% β-lg gels. Both the pure β-lg systems demonstrate a jagged growth of the crack because the β-lg structure is inhomogeneous on this length scale. The junction points between the β-lg clusters exist at irregular intervals and breaks are therefore discontinuous. A lower concentration of β-lg results in a more open aggregated structure with fewer junction points, explaining why the crack growth for the 6% β-lg gel is represented by an even more jagged curve than the one for the pure 8% β-lg gel.

Within food science, which deals with comparatively weak structures, few studies have taken up the subject of crack propagation in contrast to the sciences dealing with metals, ceramics and polymers. A study of raw and cooked carrots has shown that raw carrots fractured via rapid crack propagation through the cell walls while boiled carrots exhibited a fracture pathway track around the cells [3, 20]. Despite substantial differences in the strength of other materials, for instance polyethylene, the behaviours are still comparable. In the structure of polyethylene, which splits via discontinuous crack propagation, the pores also break up and grow far ahead of the crack tip while the continuously cracked polyethylene has a limited altered zone at the crack tip. High magnification shows a region of new developed voids as far as 500 μm ahead of the crack tip for the discontinuous crack. The fractured fibrils are much coarser after the discontinuous break-up compared to the continuous one [4]. This may be compared with our results where we also observed the formation of new pores far ahead of the crack tip for the discontinuous case and as well coarser fracture surfaces.

4. Conclusion

New possibilities have opened up within this project concerning the understanding of fracture behaviour, rheologiocally as well as microstructurally. The mini fracture cell makes it possible to observe small alterations in stress and strain because the cell is extremely sensitive (a resolution around 0.001 N) while small changes in the structure can be documented simultaneously by micrographs at high magnification. Our study shows that unique structure-rheology relationships can be revealed using this technique. For example:

- Structures formed of thin strands of particle aggregates and clusters which are relatively flexible during deformation and form many new pores before they crack have moderately high strain at fracture, ε_f, and low stress at fracture, σ_f, and discontinuous crack propagation.
- An open structure formed of poorly connected large clusters which are rigid and easily fall apart during deformation has both low ε_f and low σ_f and discontinuous crack propagation.
- A dense homogeneous structure with good connectivity is rigid during deformation and shows high σ_f and low ε_f and more continuous crack propagation.
- An open structure formed of thick network strands of clusters with good connectivity is flexible and can be deformed before cracking and shows high σ_f as well as high ε_f and discontinuous crack propagation.

Acknowledgement

This work is a part of the LiFT programme (Future Technologies for Food Production), financed by the SSF (Foundation for Strategic Research).

References

1. K. P. PLUCKNETT, S. J. POMFRET, V. NORMAND, D. FERDINANDO, C. VEERMAN, W. J. FRITH and I. T. NORTON, *J. Microsc.* **201** (2000) 279.
2. D. J. STOKES and A. M. DONALD, *J. Mater. Sci.* **35** (2000) 599.
3. B. L. THIEL and A. M. DONALD, *Annals of Botany* **82** (1998) 727.
4. V. FAVIER, T. GIROUD, E. STRIJKO, J. M. HIVER, C. G. SELL, S. HELLINCKX and A. GOLDBERG, *Polymer* **43** (2002) 1375.
5. K. NODA, A. TAKAHARA and T. KAJIYAMA, *ibid.* **42** (2001) 5803.
6. S. SARITAS, R. CAUSTON, W. B. JAMES and A. LAWLEY, *Adv. Powder, Metall. Partic. Mater.* **5** (2002) 135.
7. A. G. ATKINS and Y.-W. MAI, in "Elastic and Plastic Fracture" (Ellis Horwood Limited, England, 1985).
8. C. OLSSON, M. LANGTON and A.-M. HERMANSSON, *Food Hydrocolloids* **16** (2002b) 477.
9. C. OLSSON, M. LANGTON, M. STADING and A.-M. HERMANSSON, in "Food Colloids-Biopolymers and Materials," edited by E. Dickinson and T. van Vliet (The Royal Society of Chemistry, Cambridge, 2003) p. 26.
10. C. OLSSON, M. STADING and A.-M. HERMANSSON, *Food Hydrocolloids* **14** (2000) 473.
11. *Idem., ibid.* **16** (2002) 111.
12. S. M. FISZMAN, M. A. LLUCH and A. SALVADOR, *Intern. Dairy Journal* **9** (1999) 895.
13. M. LANGTON, in "The Microstructure of Yoghurt—a Literature Review," SIK-report No. 580 (SIK, Göteborg, 1991).

14. C. OLSSON, T. FRIGÅRD, R. ANDERSSON and A.-M. HERMANSSON, *Biomacromolecules* (2003) in press.
15. A. A. RZEPIELA, in "Deformation and Fracture Behaviour of Simulated Particulate Gels," Ph.D. Thesis, Wageningen University, Wageningen, 2003.
16. J. E. GORDON, in "Structures" (Pittman, London, 1978).
17. T. VAN VLIET, H. LUYTEN and P. WALSTRA, in "Food Polymers, Gels and Colloids No. 82," edited by E. Dickinson (Royal Society of Chemistry, Cambridge, 1993) p. 392.
18. G. E. ATTENBURROW, R. M. GOODBAND, L. J. TAYLOR and P. J. LILLFORD, *J. Cer. Sci.* **9** (1989) 61.
19. P. WALKENSTRÖM and A.-M. HERMANSSON, *Food Hydrocolloids* **8** (1994) 589.
20. P. J. LILLFORD, *MRS BULLETIN*, Dec. (2000) 38.

Received 16 September 2003
and accepted 3 June 2004